

OPTIMIZATION APPROACH FOR CATHODE EXHAUST GAS CONDITIONING OF A MULTIFUNCTIONAL PEM FUEL CELL SYSTEM FOR THE APPLICATION IN AIRCRAFT

M. Schultze, J. Horn,
 Helmut-Schmidt-University Hamburg, Institute for Control Engineering, Holstenhofweg 85,
 22043 Hamburg, Germany

Abstract

Polymer electrolyte membrane (PEM) fuel cells are highly efficient energy converters and provide electrical energy, cathode exhaust gas with low oxygen content, water and heat. Recently, fuel cells have been investigated for the use on aircraft where they have the potential of replacing the auxiliary power units (APU) that are currently used for generating electrical power during ground operations. Auxiliary power units are a significant source of noise and green house gases such as carbon dioxide. Using hydrogen fed PEM fuel cells instead has the potential of significantly reducing these pollutants.

In this study a PEM fuel cell system is investigated for generation of oxygen depleted cathode exhaust air. This gas is intended for the purpose of inerting and must have a low oxygen concentration. A nonlinear simulation model comprising the fuel cell stack, water condenser and water separators has been developed to determine operating schemes for an efficient system operation. Moreover, a spatially distributed stationary condenser model is computationally intense and therefore not adequate for fast dynamic simulations. A computationally little demanding stationary condenser model, that is based on the effectiveness NTU method, has been derived and is compared to the spatially distributed condenser model. The operating scheme derived is implemented in a Matlab/Simulink® dynamic model and simulation results are shown.

1. INTRODUCTION

Besides generation of electrical energy and water, generation of oxygen depleted cathode exhaust air (ODA) for tank inerting [1] is another central aspect of the multifunctional use of fuel cell systems. For this purpose the oxygen concentration in ODA gas must be close to or less than 10% (vol.) [2]. On aircraft auxiliary power units (APU) provide electrical power during ground operations. However, these APUs are significant sources of greenhouse gases such as CO₂ and other pollutants such as NO_x and noise. PEM fuel cells are very efficient energy converters and have the potential of significantly reducing emission of these pollutants. Among other types of fuel cells they are the most suitable for dynamic applications. They are studied as a replacement for APUs. Recently, PEM fuel cell systems have been studied for electrical power supply of autonomous robots [3] or for automotive applications [4, 5]. Operation of PEM fuel cell systems for inerting purposes has not yet been studied in detail.

Proper fuel cell system operation such as keeping the polymer membrane well humidified as well as proper supply of reactant gases and air as oxygen carrier is very central. The fuel cell system used in this study has an anode recirculation loop for a better utilization of hydrogen fuel and for gas as well as membrane humidification. A water separator is installed in the recirculation loop to prevent anode flooding, which is more likely to occur than cathode flooding [6] as the cathode gas flow continuously removes water from the cathode. Fuel and air supply as well as temperature gradient across the stack is managed by an internal fuel cell system controller. The fuel cell stack is connected to a controllable ohmic load that draws a stack current as requested. Figure 1 shows a schematic

of the multifunctional fuel cell system (MFFCS) with ODA gas conditioning in the cathode exhaust gas line. Depending on stack temperature product water partly evaporates and leaves the stack as water vapor, whereas the remaining liquid leaves the cathode as liquid water which is mostly separated by the upstream water separator (Sep. 1). In a condenser the vapor is cooled such that it condenses into liquid water, which subsequently is separated in the downstream water separator (Sep. 2).

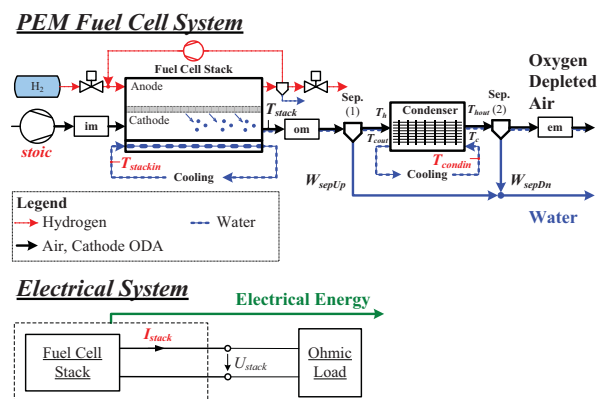


FIG 1. Schematic of the fuel cell system comprising stack, up- and downstream water separators (Sep.1,2), condenser and connecting volumes: inlet-, outlet- and exit manifold (im, om, em); H₂ is recirculated and water is removed in an anode water separator; stack and condenser are cooled by separate cooling systems

The amount of oxygen delivered exceeds the amount of oxygen required for the reaction $2H_2 + O_2 \rightarrow 2H_2O$. The oxygen excess ratio, that is termed stoichiometry (stoxic), is

a fuel cell system input parameter. Further inputs are stack current (I_{stack}), stack and condenser cooling inlet temperature ($T_{stackin}$ and T_{condin}). The fuel cell system model is based on the model reported of in [7] and is augmented by the water separators, connecting volumes and a stationary and spatially distributed condenser model, which is implemented as a cell model. The simulation model is briefly outlined in section Stationary Fuel Cell System and Condenser Model. The condenser cell model is not applicable for fast dynamic simulations. Therefore, a condenser approximation model is derived based on the cell model. Simulation results of both models are compared to each other. The error introduced by the approximation model is minor, which motivates the use of this model for fuel cell system simulation. The overall simulation model has been calibrated with experimental data. Operating schemes for an efficient PEM fuel cell system ODA-gas production are determined in section Operation Schemes for Efficient ODA Generation. A Matlab/Simulink® dynamic simulation model with the condenser approximation model is presented in section Dynamic Fuel Cell System Simulation Model and Simulation Results. The operation scheme proposed is applied to this dynamic simulation model.

2. STATIONARY FUEL CELL SYSTEM AND CONDENSER MODEL

The overall stationary simulation model comprises a model of the fuel cell system that consists of the fuel cell stack, two water separators and a water condenser in the cathode exhaust line. Inlet air is provided by a mass flow controller and a tank with pressurized air. A compressor fills the tank with dry, oil-filtered and cooled air. The stack as well as condenser cooling system is not considered in the stationary fuel cell system model. Cooling inlet temperatures are considered being constant.

2.1. Fuel Cell System Model

The fuel cell system model comprises the fuel cell stack, a mass flow controller (MFC) for cathode air supply and the anode hydrogen recirculation for better hydrogen utilization and stack humidification. The internal fuel cell system controller operates the mass flow controller such that it delivers an air mass flow as specified by stoichiometry and stack current I_{stack} drawn. Furthermore, the internal controller operates the cooling pump in the stack cooling loop to set the reference temperature difference across the fuel cell stack. Inlet air is modeled as a dry and ideal gas consisting of 21% (vol.) oxygen and 79% (vol.) nitrogen.

2.1.1. Cathode and Anode Model

The cathode is modeled as a lumped volume with a homogeneous temperature. Cathode temperature is assumed to be stack temperature. The model is derived from first principles such as mass conservation (1) for oxygen and nitrogen [4, 7]. Gases are assumed ideal and partial pressures are determined by the ideal gas law (1).

$$(1) \quad \begin{aligned} \frac{dm_{O_2}}{dt} &= W_{im,O_2} - W_{O_2,rec} - W_{ca,O_2}, & p_{O_2} &= m_{O_2} \frac{T_{stack} R_{O_2}}{V_{ca}} \\ \frac{dm_{N_2}}{dt} &= W_{im,N_2} - W_{ca,N_2}, & p_{N_2} &= m_{N_2} \frac{T_{stack} R_{N_2}}{V_{ca}} \end{aligned}$$

Condensation is assumed to occur instantaneously and water is transported out of the cathode as vapor and liquid. Water also diffuses through the membrane to the anode. The membrane model is given in [4, 7]. To prevent anode flooding a water separator removes water from the hydrogen gas flow in the anode recirculation loop, in which a compressor recirculates hydrogen gas. When considering the fuel cell stack outlet water mass flows, the anode water removal for this fuel cell system type cannot be neglected. Therefore, as proposed by [5] the anode model has been extended by a term for anode water removal (2) with separation efficiency $\eta_{sep,an}$ and the hydrogen compressor maximum mass flow $W_{recirc,max}$ with $m_{H_2O,an}$ being the mass of water and $m_{H_2,an}$ the mass of hydrogen in the anode and membrane water flow W_{mem} (3).

$$(2) \quad W_{sep,an} = \eta_{sep,an} W_{recirc,max} \frac{m_{H_2O,an}}{m_{H_2O,an} + m_{H_2,an}}$$

$$(3) \quad \frac{dm_{H_2O,an}}{dt} = -W_{mem} - W_{sep,an}$$

The hydrogen recirculation pump speed increases with stack current. The higher the hydrogen mass flow in the recirculation line, the more water can be separated. Furthermore, separation efficiency depends on the separator temperature as the separator partially functions as a condenser. An empirical approach (4) has been chosen to describe the water separation efficiency in terms of stack current. The anode recirculation loop water separation efficiency can be adjusted by k_1 and k_2 .

$$(4) \quad \eta_{sep,an} = \exp(k_1 + k_2 I_{stack})$$

2.1.2. Stack Thermal Model

Fuel cell stack temperature T_{stack} is obtained by energy conservation (5) with stack heat capacity C_{st} . The energy flows are given by chemical energy provided by hydrogen (higher heating value HHV), electrical energy delivered by the stack and thermal energy flows of ODA-gas, liquid water and water vapor. Anode water separation mass flow $W_{sep,an}$ is taken into account as well. Energy conservation (5) is obtained using stack cooling inlet temperature $T_{stackin}$, cooling mass flow W_{cool} , feed air mass flow W_{im} from inlet manifold with temperature T_{im} , ODA mass flow W_{oda} and $W_{odacell} = W_{oda}/n_{cells}$ as the ODA mass flow per cell, liquid $W_{ca,l}$ and vapor mass flow $W_{ca,v}$ leaving the stack. The specific heat capacities are c_{cool} , c_{air} , c_{oda} , c_l , c_v and h_0 being the enthalpy of evaporation of water. The number of cells in the fuel cell stack is n_{cells} .

$$(5) \quad \begin{aligned} C_{st} \frac{dT_{st}}{dt} &= (1.48 n_{cells} - U_{stack}) I_{stack} + W_{cool} c_{cool} (T_{stackin} - T_{stack}) \\ &+ W_{im} c_{air} (T_{im} - T_0) - W_{oda} c_{oda} (T_{stack} - T_0) \\ &- W_{ca,l} c_l (T_{stack} - T_0) - W_{ca,v} (h_0 + c_v (T_{stack} - T_0)) \\ &- W_{sep,an} c_l (T_{stack} - T_0) \end{aligned}$$

2.1.3. Outlet- and Exit Manifold Model

Compared to [7] the fuel cell system model is extended by an exit manifold model. The cathode exhaust gas cools down in the outlet manifold, such that the outlet manifold temperature T_{om} is lower than stack temperature T_{stack} , which is accounted for by a constant temperature loss $T_{om} = T_{stack} - T_{om,loss}$. The dynamic outlet manifold model in [7] has states for ODA and water mass residing in the manifold. However, keeping the number of states low is

highly favorable. Model reduction can be achieved by approximating the water dynamics in the outlet- and exit manifold by a static behavior. This is reasonable as it is not measurable how much liquid water is residing in the manifold. ODA-gas still has a temperature of 50-70°C in the outlet manifold. So simply neglecting the vapor or liquid water mass flows would be inaccurate. However, as enough liquid water is carried by the gas stream, a relative humidity of 100% can be assumed despite of the pressure loss across the manifold. Therefore, the vapor pressure can be considered saturation vapor pressure p_v^{sat} . Outlet manifold vapor outlet mass flow $W_{om,v}$ is determined by water loading X_{om} , however, the vapor mass flow cannot exceed the inlet mass flow of vapor and liquid from cathode $W_{ca,v}$ and $W_{ca,l}$. Therefore, the vapor mass flow is taken as the minimum of inlet mass flow and maximum possible mass flow. The remainder is liquid water $W_{om,l}$ (6). Water loading is $X_{om} = p_v^{sat}/(p_{om}-p_v^{sat}) * R_{oda}/R_v$ with the vapor gas constant R_v and R_{oda} the ODA gas constant being approximated by the gas constant of air R_{air} . The flow that establishes at the outlet manifold exit is a turbulent flow and is therefore modeled as given by (7) with the flow constant c_{sep1} and the pressure gradient of outlet manifold p_{om} and condenser inlet pressure $p_{cond,in}$. Outlet manifold pressure is obtained by $p_{om} = p_v^{sat} + p_{om,oda}$.

$$(6) \quad W_{om,v} = \min(X_{om}W_{om,oda}, W_{ca,v} + W_{ca,l})$$

$$W_{om,l} = W_{ca,v} + W_{ca,l} - W_{om,v}$$

$$(7) \quad W_{om} = c_{sep1} \sqrt{(p_{om} - p_{cond,in})}$$

$$(8) \quad \frac{dm_{om,oda}}{dt} = W_{ca,oda} - \frac{1}{1 + X_{om}} W_{om}, \quad p_{om,oda} = m_{om,oda} \frac{T_{om} R_{oda}}{V_{om}}$$

The same applies for the exit manifold. Here, not enough liquid water might be present to guarantee a fully saturated flow. Outlet temperature during operation is less than 40°C due to cooling in the condenser. The vapor pressure of a fully saturated ODA flow is less than 7% as shown in table 1, therefore, the error introduced is minor. The vapor mass flow for fully saturated flow is less than 5% of the ODA mass flow. The vapor saturation pressure is calculated as in [7, 8]. Exit manifold pressure is close to ambient pressure, which is assumed as $p=101325$ Pa.

Temp. in °C	Vapor saturation pressure p_v^{sat} in Pa	Pressure ratio p_v^{sat}/p in %	Water loading in %
5	872.8	0.9	0.5
10	1228.7	1.2	0.8
20	2339.9	2.3	1.5
30	4246.4	4.2	2.7
40	7382.3	7.3	4.9

TAB 1. Pressure ratio and water loading for different manifold temperatures leading to vapor saturation pressure p_v^{sat} for 100% saturation; p is 101325Pa

The flow establishing at exit manifold outlet W_{em} is turbulent and is modeled according to (7) with flow constant c_{em} and pressure difference of exit manifold and ambient ($p_{em} - p_{amb}$). Fluid flow into the exit manifold is modeled as turbulent assuming that vapor mass flow is small compared to ODA mass flow through the downstream separator. So, ODA mass flow $W_{sep2,oda}$ into the exit manifold is gained by (9) with constant c_{sep2} and pressure difference of condenser outlet $p_{cond,out}$ and p_{em} .

$$(9) \quad W_{sep2,oda} = c_{sep2} \sqrt{(p_{cond,out} - p_{em})}$$

2.1.4. Water Separator Model

Upstream and downstream cyclone water separators (Sep. 1, 2) are modeled equivalently. They have a low pressure loss, such that condensation or evaporation inside the separators can be neglected. Their separation efficiency is $\eta_{separator} = 99\%$ and they are implemented as static models. Equations for the upstream separator are (10). A water mass flow of W_{sepUp} is removed from the gas flow. The mass flows of liquid and vapor from the condenser outlet enter the downstream separator, where a water mass flow of W_{sepDn} (11) is removed from the gas flow.

$$(10) \quad W_{sep1,v} = W_{om,v}$$

$$W_{sep1,l} = (1 - \eta_{separator}) \cdot W_{om,l}$$

$$W_{sepUp} = \eta_{separator} \cdot W_{om,l}$$

$$(11) \quad W_{sep2,v} = W_{cond,v}$$

$$W_{sep2,l} = (1 - \eta_{separator}) \cdot W_{cond,l}$$

$$W_{sepDn} = \eta_{separator} \cdot W_{cond,l}$$

2.1.5. Compressor Power Model

For generation of the feed air mass flow the compressor consumes electrical power. Here, the power needed for compressing air [4] from ambient pressure p_{amb} to inlet manifold pressure p_{im} is determined by thermodynamic equation (12). The feed air mass flow is obtained by stack current and stoichiometry. The compressor efficiency is assumed to be $\eta_{cpr} = 70\%$ [9] and the compressor motor efficiency is assumed to be $\eta_{cprmotor} = 97\%$.

$$(12) \quad P_{cpr} = \frac{1}{\eta_{cprmotor}} \frac{1}{\eta_{cpr}} c_{p,air} T_{amb} \left(\left(\frac{p_{im}}{p_{amb}} \right)^{\frac{\kappa-1}{\kappa}} - 1 \right) W_{air}$$

2.1.6. System Efficiency

Chemical power provided by hydrogen (13) as chemical energy over time is determined by the higher heating value (HHV), which translates into a virtual cell voltage of 1.48V.

$$(13) \quad P_{chem} = I_{stack} \cdot 1.48V \cdot n_{cells}$$

The fuel cell system does not power the air compressor. However, power being consumed for air compression is significant and therefore needs to be taken into account for system efficiency consideration. The power consumed by the multifunctional fuel cell system is approximated by the sum of chemical power provided by hydrogen and the power needed for generating mass flow of compressed air (12). Power consumption of cooling pumps, valves, fans etc. is neglected as their power demand is low compared to the compressor power. To generate a specific ODA mass flow, stack current has to be drawn. The stack voltage settles depending on stack current and stoichiometry. Electrical power $P_{stack} = I_{stack} U_{stack}$ is generated and consumed by the electrical load. It is favorable to exhibit a high system efficiency and hence to convert as much chemical energy into electrical energy as possible to save costly fuel. Efficiency is gained as the ratio of electrical stack power and sum of chemical and compressor power supplied to the fuel cell system (14).

$$(14) \quad \eta_{system} = \frac{P_{stack}}{P_{cpr} + P_{chem}}$$

2.1.7. Voltage Model

Stack voltage $U_{stack} = n_{cells} U_{cell}$ is the sum of all n_{cells} cell voltages. Cell voltage is modeled as $U_{cell} = U_{rev} - \eta_{act} - \eta_{\Omega}$ (15) with the reversible cell voltage U_{rev} , activation loss η_{act} [10] and ohmic loss η_{Ω} [11]. The membrane thickness is given by d_m and the active surface area by A_{sfc} . Parameters ζ_1, \dots, ζ_4 and b_1, \dots, b_3 have been identified.

$$(15) \quad U_{rev} = 1.229 - 0.85 \cdot 10^{-3} (T_{stack} - 298.15) + 4.3 \cdot 10^{-5} T_{stack} \left(\ln \frac{p_{H_2}}{p_0} + \frac{1}{2} \ln \frac{p_{O_2}}{p_0} \right)$$

$$\eta_{act} = \zeta_1 + \zeta_2 T_{stack} + \zeta_3 T_{stack} \ln \left(p_{O_2} e^{(498/T_{stack})} / 5.08 \cdot 10^{-6} \right) + \zeta_4 T_{stack} \ln(I_{stack})$$

$$\eta_{\Omega} = \frac{d_m}{(h_m^2 - b_2)} e^{-b_1 \left(\frac{1}{303} - \frac{1}{T_{stack}} \right)} \frac{I_{stack}}{A_{sfc}}$$

An exemplary polarization curve [7] is shown in figure 2. For increasing stack currents stack voltage decreases. Moreover, stack voltage can be increased for constant stack current when stoichiometry is increased, which leads to an increase in oxygen partial pressure in the fuel cell stack cathode leading to reduced voltage losses.

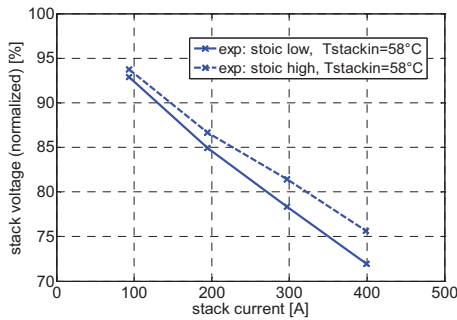


FIG 2. Example polarization curve [7] for high and low stoic and stack cooling inlet temperature 58°C

2.2. Condenser Model

Two stationary counter-flow condenser models are compared in the following. For dynamic simulation of the fuel cell system a fast condenser simulation model is desirable. The condenser cell model proposed first, however, is not applicable for such simulations as it takes too long to solve. Based on the cell model an approximation model is derived. It is solved much faster and is applicable for dynamic fuel cell system simulations.

2.2.1. Condenser Cell Model

The condenser is modeled as schematically shown in figure 3 with length 1 and n identical cells. For simulation $n=50$ is set. The overall heat transfer coefficient UA is assumed constant throughout the whole condenser. Condenser fouling and heat transfer reduction resulting from water condensation is being neglected. Cell heat transfer coefficient is determined by dividing UA by the number of cells as $ua=UA/n$. Mass and energy conservation is applied to each of the cells. The heat transferred from condenser ODA side to cooling side is driven by the temperature difference of mean ODA cell $T_{h,i}$ and mean cooling cell temperature $T_{c,i}$ as follows (16).

$$(16) \quad \dot{Q}_i = ua \left(\frac{1}{2} (T_{h,i} + T_{h,i+1}) - \frac{1}{2} (T_{c,i} + T_{c,i+1}) \right)$$

$$(17) \quad 0 = W_{cool} c_c T_{c,i+1} - W_{cool} c_c T_{c,i} + \dot{Q}_i$$

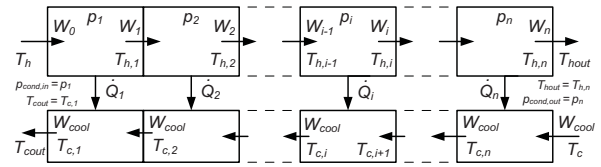


FIG 3. Condenser cell model: mass and energy balance for each cell: ODA side (top cells) and cooling side (bottom cells)

On the cooling side a constant and incompressible mass flow W_{cool} is applied. The energy balance of the cooling side is given by (17).

On the ODA side a compressible and turbulent fluid flow is assumed. The mass flow leaving a cell is given as $W_i = k^* \sqrt{p_i - p_{i+1}}$ by coefficient k^* and pressure difference across two adjacent cells. ODA mass flow and vapor mass flow of cell i are governed by (18) with water loading X_i (19) obtained using cell temperature $T_{h,i}$. A fully saturated flow is assumed to leave each cell.

$$(18) \quad W_{oda,i} = \frac{1}{1 + X_i} W_i$$

$$W_{v,i} = \frac{X_i}{1 + X_i} W_i$$

$$(19) \quad X_i = \frac{p_v^{sat}(T_{h,i})}{p_i - p_v^{sat}(T_{h,i})} \frac{R_{oda}}{R_v}$$

Mass and energy conservation across one cell lead to equations (20) and (21) with $W_{l,i}$, $W_{v,i}$ and W_{oda} being the mass flow of liquid, vapor and ODA-gas, respectively.

$$(20) \quad 0 = W_{oda,i} - W_{oda,i+1}$$

$$W_{l,i+1} = W_{v,i} + W_{l,i} - W_{v,i+1}$$

$$(21) \quad 0 = W_{oda,i} c_{oda} T_{h,i} + W_{v,i} (h_0 + c_v T_{h,i}) + W_{l,i} c_l T_{h,i}$$

$$- W_{oda,i+1} c_{oda} T_{h,i+1} - W_{v,i+1} (h_0 + c_v T_{h,i+1})$$

$$- W_{l,i+1} c_l T_{h,i+1} - \dot{Q}_i$$

The cooling outlet temperature T_{cool} is obtained by the temperature $T_{c,1}$ of cooling cell 1 as $T_{cool} = T_{c,1}$. At the ODA side, vapor and liquid mass flow at the inlet are prescribed by the upstream water separator. The outlet temperature T_{hout} is taken as temperature $T_{h,n}$ of cell n as $T_{hout} = T_{h,n}$. Condenser inlet pressure is taken as the pressure in cell 1 $p_{cond,in} = p_1$ and condenser outlet pressure is taken as pressure in cell n $p_{cond,out} = p_n$. $T_{c,i}$, $T_{h,i}$ and p_i are the unknowns leading to a total count of $3x$ number of condenser-cells. Fuel cell system and condenser model unknowns are solved for by a Newton-Raphson Algorithm.

2.2.2. Condenser Approximation Model

In the following a differential and stationary model of a counter flow condenser as shown in figure 4 is used to derive an approximation model. The model is based on the effectiveness-NTU method [12]. NTU is the number of transfer units, which is an important parameter in heat exchanger modeling. Heat transfer coefficient of a differential element is U . The model assumes that ODA-gas enters and leaves the condenser with a saturation of 100% and is fully saturated inside the condenser. ODA-gas, vapor and liquid have the same temperature.

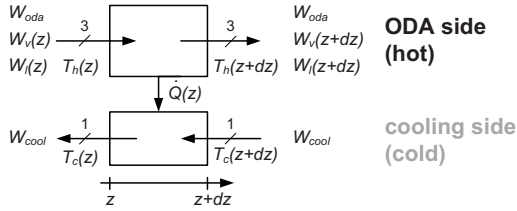


FIG 4. Condenser differential model: mass and energy balance for a differential element

Modeling heat transferred from ODA side to cooling side as (22) and neglecting higher order terms leads to (23).

$$(22) \dot{Q}(z) = Udz \left(\frac{1}{2}(T_h(z) + T_h(z+dz)) - \frac{1}{2}(T_c(z) + T_c(z+dz)) \right)$$

$$(23) \dot{Q}(z) = Udz(T_h(z) - T_c(z))$$

The energy balance across a cooling cell is given by (24) and transforms into (25) when applying a Taylor series expansion and neglecting higher order terms.

$$(24) 0 = W_{cool}c_c T_c(z+dz) - W_{cool}c_c T_c(z) + \dot{Q}(z)$$

$$(25) W_{cool}c_c \frac{\partial T_c}{\partial z} = C_c \frac{\partial T_c}{\partial z} = -U(T_h(z) - T_c(z))$$

The mass flow of ODA is assumed constant. The condenser pressure is modeled as a constant mean pressure p_c governed by the arithmetic mean of condenser inlet and outlet pressure (26).

$$(26) p_c = \frac{1}{2}(p_{cond,in} + p_{cond,out})$$

Water loading of fully saturated ODA is modeled as (27) and using the temperature of ODA $T_h(z)$.

$$(27) X(z) = \frac{p_v^{sat}(T_h(z))}{p_c - p_v^{sat}(T_h(z))} \frac{R_{oda}}{R_v}$$

The energy balance at the ODA side is as follows (28).

$$(28) 0 = W_{oda}c_{oda}T_h(z) + W_v(z)(h_0 + c_v T_h(z)) + W_l(z)c_l T_h(z) - W_{oda}c_{oda}T_h(z+dz) - W_v(z+dz)(h_0 + c_v T_h(z+dz)) - W_l(z+dz)c_l T_h(z+dz) - Udz(T_h(z) - T_c(z))$$

Applying a Taylor series expansion and neglecting higher order terms reduces (28) further leading to (29).

$$(29) 0 = -W_{oda}c_{oda} \frac{\partial T_h}{\partial z} dz - h_0 \frac{\partial W_v}{\partial z} dz - Udz(T_h(z) - T_c(z)) - c_v \left(W_v(z) \frac{\partial T_h}{\partial z} dz + \frac{\partial W_v}{\partial z} T_h(z) dz \right) - c_l \left(W_l(z) \frac{\partial T_h}{\partial z} dz + \frac{\partial W_l}{\partial z} T_h(z) dz \right)$$

Exploiting differentiation of $W_v(z) = X(z)W_{oda}$ with respect to

z leads to $\frac{\partial W_v(z)}{\partial z} = \frac{\partial X(z)}{\partial z} W_{oda}$. The water mass balance

across one cell leads to $\frac{\partial W_l(z)}{\partial z} = -\frac{\partial W_v(z)}{\partial z}$. Considering that

(29) is dominated by the enthalpy of evaporation h_0 , equation (29) can further be reduced. The derivative of water loading with respect to z is obtained by (30).

$$(30) \frac{\partial X(z)}{\partial z} = \frac{\partial X(T_h(z))}{\partial z} = \frac{\partial X(T_h)}{\partial T_h} \frac{\partial T_h(z)}{\partial z}$$

Derivative of water loading with respect to temperature is approximated as the derivative at mean ODA temperature $T_{h,mean}$ in the condenser (31). Mean temperature is gained

as the arithmetic mean of ODA in- and outlet temperature $T_{h,mean} = 1/2 (T_{hout} + T_h)$. This leads to differential equation (32) on the ODA side of the condenser.

$$(31) \frac{\partial X}{\partial T} \approx \frac{\partial X}{\partial T} \Big|_{T_{h,mean}} = \frac{dp_v^{sat}}{dT} \Big|_{T_{h,mean}} \cdot \frac{p_c}{(p_c - p_v^{sat}(T_{h,mean}))^2} \frac{R_{oda}}{R_v}$$

$$(32) \left(h_0 W_{oda} \frac{\partial X}{\partial T} \Big|_{T_{h,mean}} \right) \frac{\partial T_h}{\partial z} = C_h \frac{\partial T_h}{\partial z} = -U(T_h(z) - T_c(z))$$

Model equations of the cooling side and equations of the ODA side are similar to model equations of a counter-flow heat exchanger with incompressible mass flows. Therefore, the effectiveness NTU method [12] is applied. Condenser outflow temperature is governed as (33).

$$(33) T_{hout} = f(T_{hout}) = T_h - \varepsilon \cdot C_{min} / C_h \cdot (T_h - T_c)$$

The heat capacity flow C_c of the coolant is much higher than C_h . Hence, the minimum heat capacity flow could be approximated as $C_{min} = \min(C_c, C_h) = C_h$ (34). Nevertheless, condenser ODA outlet temperature is determined by (33).

$$(34) T_{hout} = T_h - \varepsilon \cdot C_h / C_h \cdot (T_h - T_c) = T_h - \varepsilon(T_h - T_c)$$

Effectiveness ε is calculated using the equation for a counter-flow heat exchanger (35) based on the effectiveness NTU method [12] with $C_{min} = \min(C_h, C_c)$, $C_{max} = \max(C_h, C_c)$, $C^* = C_{min} / C_{max}$ and $NTU = UA / C_{min}$.

$$(35) \varepsilon = \frac{1 - \exp(-NTU(1 - C^*))}{1 - C^* \exp(-NTU(1 - C^*))} \text{ for } C^* \neq 1 \text{ and } \varepsilon = \frac{NTU}{1 + NTU} \text{ for } C^* = 1$$

As the actual ODA outlet temperature T_{hout} is used to compute $\partial X / \partial T$ at the mean temperature as well as C_h , it is obvious that T_{hout} is given by an implicit equation (33). A fixed-point iteration (36) is used to solve this equation. Iteration starts with cooling inlet temperature $T_{hout,0} = T_c$ as initial guess for ODA side outlet temperature.

$$(36) T_{hout,k+1} = f(T_{hout,k}) = T_h - \varepsilon_k \frac{C_{min,k}}{C_{h,k}} (T_h - T_c)$$

The outlet temperature is used to calculate the mass flow of vapor $W_{v,out} = X(T_{hout})W_{oda}$ and liquid leaving the condenser $W_{l,out} = W_{l,in} + W_{v,in} - W_{v,out}$ with the water loading calculated at outlet temperature T_{hout} . According to (21) an energy balance about the ODA side of the condenser delivers the heat flow transferred to the cooling side. According to (17) this heat flow is taken to obtain the cooling outlet temperature T_{cout} .

The fixed-point iteration (36) converges for $\left| \frac{df(T_{hout})}{dT_{hout}} \right| < 1$.

Function value f and its derivative with respect to temperature T_{hout} have been determined and plotted over T_{hout} in figure 5. Calculations were done for typical values of pressure, ODA mass flow and temperature occurring during fuel cell system operation. Values are mean pressure $p_c = 1.0$ and 1.3 bar, ODA mass flow of $W_{odacell} = 0.03, 0.07, 0.20$ and 0.27 g/s/cell, inlet temperature $T_h = 40$ and 65°C and cooling temperature $T_c = 5$ and 20°C . As shown in figure 5 the fixed-point iteration convergence condition is satisfied. The derivative with respect to T_{hout} is greater than 0 and less than 1.

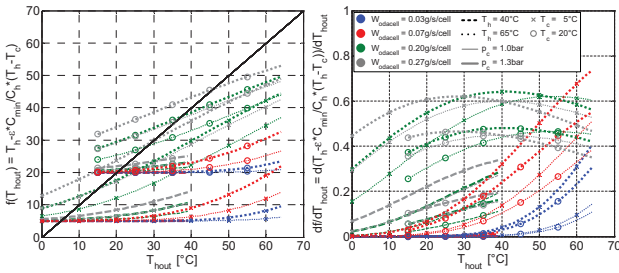


FIG 5. Function f over temperature T_{hout} (left) and derivative df/dT_{hout} over T_{hout} (right)

After 4-5 steps the fixed-point iteration has reached the solution. The iteration's speed of convergence can be increased by relaxing the original fixed-point iteration $T_{hout,k+1} = f(T_{hout,k})$ by a constant function r to $T_{hout,k+1} = g(T_{hout,k}) = rT_{hout,k} + (1-r)f(T_{hout,k})$. The constant has been chosen as $r = -0.5$ to lower the absolute value of the derivative of $g(T_{hout})$ with respect to T_{hout} . As shown in figure 6 the relaxed fixed-point iteration takes 2 steps until the solution has been reached.

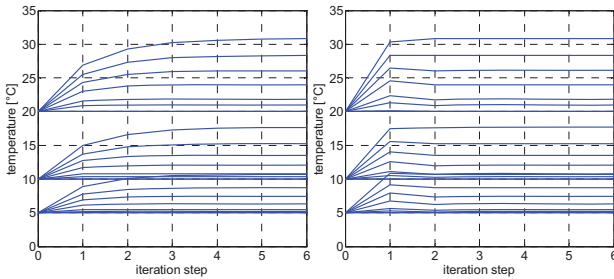


FIG 6. Speed of convergence for fixed-point iteration without (left) and with relaxation (right)

2.2.3. Condenser Model Comparison and Approximation Model Implementation

The fuel cell system model containing the condenser cell model was simulated for stack currents of 100, 200, 300 and 400A, stoichiometry of 1.7 and 2.0, condenser cooling temperatures of 5, 10 and 20°C and heat transfer coefficient $UA=400W/K$. Stack cooling is less problematic for high temperature gradients, so the stack is cooled with inlet temperature of 58°C to gain a high temperature gradient. Model parameters such as for polarization curve and mass flows have been determined as reported in [7]. Comparing the condenser approximation model to the cell model was done by taking the fuel cell system simulation model condenser inlet parameters such as ODA, vapor and liquid mass flows as well as ODA and cooling inlet temperature and prescribing them to the condenser approximation model. Subsequently, ODA-gas outlet temperature and heat flow transferred from hot to cooling side were computed with the condenser approximation model. A comparison of the model results is shown in figure 7. The heat flow approximation error e_{dQ} is obtained as the ratio $e_{dQ} = (dQ_{cond,cell} - dQ_{cond,approx.})/dQ_{cond,cell}$ with the heat flow $dQ_{cond,cell}$ calculated by the cell model and heat flow $dQ_{cond,approx}$ determined by the approximation model. Error in approximating the ODA outlet temperature as well as error in the heat flow transferred is little. Motivated by the small error on outlet temperature and heat flow transferred, the condenser approximation model is used for the simulation model presented in the following.

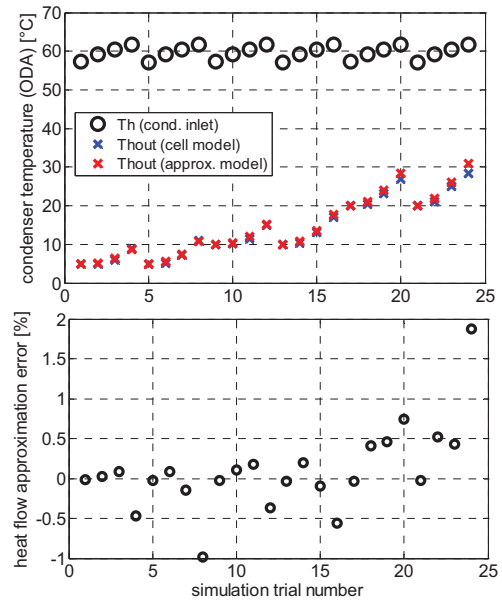


FIG 7. Condenser ODA outlet temperature: cell and approximation model (top); heat flow error e_{dQ} of cell and approximation model (bottom)

2.3. Approximation Model Implementation

For fast fuel cell system simulations and for the purpose of dynamic simulations the condenser cell model has been replaced by the condenser approximation model. Implementation in the simulation model is presented in the following paragraph.

2.3.1. Approximation Model Mass Flows

Equations for the ODA and vapor mass flows through the separator-condenser-separator unit are obtained in the following. The mass flow through the entire unit is modeled to depend on the pressure difference ($p_{om} - p_{em}$) of outlet end exit manifold. The vapor mass flow through the upstream water separator is governed by the water loading X_{om} in the outlet manifold leading to (37).

$$(37) (1 + X_{om})^2 W_{oda}^2 = c_{sepl}^2 (p_{om} - p_{cond,in})$$

The total mass flow through the downstream condenser is approximated as a pure ODA mass flow (9) as most of the vapor has condensed. Equation (9) leads to (38).

$$(38) W_{oda}^2 = c_{sep}^2 (p_{cond,out} - p_{em})$$

Vapor condenses as it travels through the condenser. This leads to an increase of the flow resistance. Further, the flow through the condenser can be considered turbulent. To account for the turbulent flow that also depends on the mass flow of water carried, the mass flow through the condenser is modeled as an ODA and vapor mass flow. As the vapor mass flow is assumed not to change across the upstream water separator, the condenser inlet vapor mass flow is modeled as the vapor mass flow $W_{om,v} = X_{om} W_{oda}$ leaving the outlet manifold and entering the upstream water separator. Therefore, the ODA mass flow through the condenser is obtained by (39).

$$(39) (1 + X_{OM})^2 W_{oda}^2 = c_{cond}^2 (p_{cond,in} - p_{cond,out})$$

Mass flow of ODA-gas through the entire unit is governed

by equations (37), (38) and (39) as follows.

$$(40) \quad W_{oda} = \frac{\sqrt{P_{om} - P_{em}}}{\sqrt{\frac{(1+X_{om})^2}{c_{sep1}^2} + \frac{(1+X_{om})^2}{c_{cond}^2} + \frac{1}{c_{sep2}^2}}}$$

2.3.2. Approximation Model Temperatures

The condenser outlet temperature T_{hout} is calculated with the mean pressure (26) and the approximation condenser model with relaxation for faster convergence of the solution. Vapor and liquid mass flow at condenser inlet are prescribed as $W_{cond,v,in}=W_{om,v}$ and $W_{cond,l,in}=W_{sep1,l}$. Vapor outlet mass flow $W_{cond,v,out}$ is determined through the condenser outlet water loading assuming a fully saturated flow at mean pressure and at temperature T_{hout} . Liquid water mass flow $W_{cond,l,out}$ at the outlet is determined through a stationary condenser water balance. Stationary energy balances of ODA (41) and cooling side (42) lead to the cooling outlet temperature T_{cout} . The model iteration is set to four steps to gain a fast and close solution.

$$(41) \quad \begin{aligned} 0 = & W_{oda} c_{oda} T_h + W_{cond,v,in} (h_0 + c_v T_h) + W_{cond,l,in} c_l T_h \\ & - W_{oda} c_{oda} T_{hout} - W_{cond,v,out} (h_0 + c_v T_{hout}) \\ & - W_{cond,l,out} c_l T_{hout} - \dot{Q}_{cond} \end{aligned}$$

$$(42) \quad 0 = W_{cool} c_{cool} (T_c - T_{cout}) + \dot{Q}_{cond}$$

3. OPERATION SCHEMES FOR EFFICIENT ODA GENERATION

The fuel cell system consisting of the fuel cell stack, water separation unit und cooling systems shall be operated to deliver oxygen depleted air being conditioned with respect to water loading and oxygen content. To save costly fuel an efficient generation of ODA-gas is favorable.

A reference ODA mass flow can be obtained by different combinations of stoichiometry and stack current as is obvious by a stationary mass flow balance about the stack cathode. Feed air mass flow $W_{air,MFC}$ (43) is provided by the mass flow controller (MFC). The oxygen mass flow consumed $W_{O2,react}$ by the chemical reaction (44) reduces the feed air mass flow and leads to the ODA mass flow W_{oda} (45). Volumetric ODA oxygen content c_{O2} is the ratio of oxygen partial pressure to the sum of oxygen and nitrogen partial pressure (1) in the cathode (46).

$$(43) \quad W_{air,MFC} = \frac{I_{stack}}{4F} n_{cells} \lambda \left(M_{O2} + \frac{0.79}{0.21} M_{N2} \right)$$

$$(44) \quad W_{O2,react} = \frac{I_{stack}}{4F} n_{cells} M_{O2}$$

$$(45) \quad W_{oda} = \frac{I_{stack}}{4F} n_{cells} \left((\lambda - 1) M_{O2} + \lambda \frac{0.79}{0.21} M_{N2} \right)$$

$$(46) \quad c_{O2} = \frac{P_{O2}}{P_{O2} + P_{N2}}$$

For inerting the ODA flow must have an oxygen content of close to 10%. Generally, oxygen content of the cathode exhaust gas could be brought to zero, if the oxygen excess ratio of the feed air was 1. However, this would cause oxygen starvation in the cathode and could severely damage the fuel cell stack [13]. If the oxygen excess ratio is greater than 1, then not all oxygen is consumed by the chemical reaction and an oxygen content of greater than

zero will establish in the cathode exhaust gas. So, the choice of oxygen excess ratio determines the stationary oxygen concentration in ODA-gas. Stationary volumetric O_2 concentration of ODA-gas (46) can also be obtained as the ratio of molar flows (47) of oxygen and nitrogen leaving the fuel cell stack with $N_{O2out} = n_{cells} / (4F) (\lambda - 1) I_{stack}$ and $N_{N2out} = 0.79 / 0.21 n_{cells} / (4F) \lambda I_{stack}$. Equation (47) is solved for λ to determine the static stoichiometry input required to gain the reference ODA oxygen concentration $c_{O2,ref}$ (48).

$$(47) \quad c_{O2} = \frac{N_{O2out}}{N_{O2out} + N_{N2out}} = \frac{\lambda - 1}{\lambda(1 + 0.79/0.21) - 1}$$

$$(48) \quad \lambda = \frac{c_{O2,ref} - 1}{c_{O2,ref} (1 + 0.79/0.21) - 1}$$

Besides correctly conditioning ODA, the reference mass flow $W_{oda,ref}$ has to be provided. ODA mass flow depends on stack current I_{stack} and cathode stoichiometry λ . Assuming constant stoichiometry, e.g. $\lambda = 1.72$, and solving equation (45) for stack current I_{stack} , a relation of reference ODA mass flow to stack current is derived as follows.

$$(49) \quad I_{stack} = W_{oda,ref} \frac{4F}{n_{cells} ((\lambda - 1) M_{O2} + \lambda (0.79/0.21) M_{N2})}$$

An important parameter is the amount of water carried by ODA-gas. The ratio of water mass flow to dry ODA mass flow is termed ODA water loading and has units of g/kg. In the fuel cell system model water loading is gained as the ratio of the sum of vapor $W_{em,v}$ and liquid $W_{em,l}$ mass flow to dry ODA mass flow $W_{em,oda}$ in the exit manifold (50).

$$(50) \quad X_{oda,em} = (W_{em,v} + W_{em,l}) / (W_{em,oda}) \times 1000$$

3.1. Stationary Simulation Model

The condenser model of the stationary fuel cell system simulation model utilized in the following is implemented as the approximation model based on the effectiveness-NTU method. The condenser is considered to exhibit high cooling, which is modeled by a high heat transfer coefficient. ODA outlet temperature then is close to the condenser cooling inlet temperature. Therefore, in contrast to simulations shown in figure 7, a value of $UA=600W/K$ is taken for the condenser model of the stationary fuel cell system simulation model. The fuel cell system was simulated for stack currents, stack cooling inlet temperature, stoichiometry and condenser cooling temperature as given in Section Condenser Model Comparison. Simulation results are shown in figure 8.

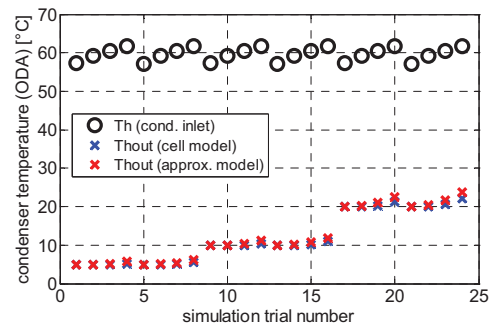


FIG 8. Condenser outlet temperature for cell model and approximation model for different sets of system inputs and $UA=600W/K$

3.2. Condenser Operation: ODA Water Loading

To investigate water loading of oxygen depleted air at different condenser cooling temperatures, the stationary fuel cell system has been simulated for condenser inlet temperatures $T_{condin} = 5, 7.5 \dots 20^\circ\text{C}$, ODA cell mass flows $W_{odacell} = 0.07, 0.13$ and 0.20g/s/cell and stoichiometries of $\lambda = 1.5, 1.7$ and 2.0 . Stack current I_{stack} was determined by equation (49). Simulation results are shown in figure 9.

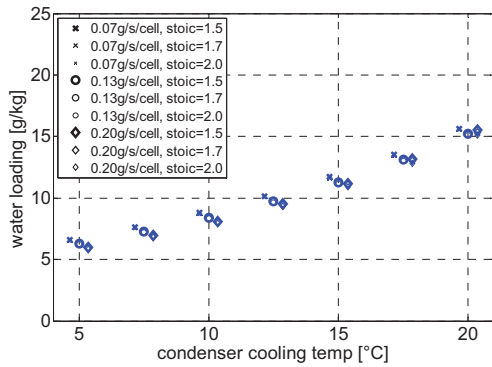


FIG 9. Simulation: ODA water loading in exit manifold for condenser cooling inlet temperatures 5, 7.5...20°C, cell mass flows 0.07, 0.13, 0.20g/s/cell and stoic. 1.5, 1.7, 2.0

Water loading rises with increasing condenser cooling temperature. This is plausible as for lower temperature more water vapor condenses into liquid, which is removed by the down-stream water separator, subsequently. At constant cooling temperature and for different ODA mass flows water loading only changes slightly. The influence of stoichiometry on water loading for constant ODA mass flow is weak and is due to the influence of stoichiometry on stack temperature. To achieve a very low water loading, the condenser would have to be cooled at its minimum cooling inlet temperature of 5°C. For less restrictive limitations on ODA water loading, the condenser inlet cooling temperature can be increased. Using this type of condenser a water loading of 15g/kg is gained at a condenser inlet cooling temperature of 20°C. For inerting it is desired to have low water loading. To remove most of the water carried, the condenser is cooled with 5°C.

3.3. Fuel Cell System Stack Operation

The fuel cell system model has been simulated for a condenser inlet cooling temperature of $T_{condin} = 5^\circ\text{C}$ and stoichiometry of 1.5 - 2.1. Stack currents were determined by (49) to generate ODA cell mass flows of 0.07, 0.13 and 0.20g/s/cell. Results are shown in figures 10, 11 and 12.

As outlined previously, the system parameter stoichiometry affects the stationary ODA-gas oxygen content. Figure 10 depicts the stationary ODA-gas oxygen content plotted against stoichiometry. When the fuel cell system is operated at stoichiometry 1.72, an ODA oxygen content of close to 10% is gained. As shown in figure 11 the stack current required for a constant ODA mass flow decreases with increasing stoichiometry, which is plausible as more air is fed to the fuel cell stack for increasing stoichiometry. For the operation of the fuel cell system, however, not the entire range of stack currents shown in figure 11 is applicable. For this fuel cell stack, a stack

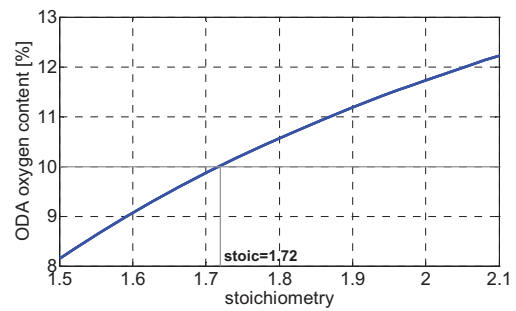


FIG 10. Stationary oxygen content of oxygen depleted air plotted over cathode stoichiometry; a 10% O₂-content is obtained for stoichiometry 1.72

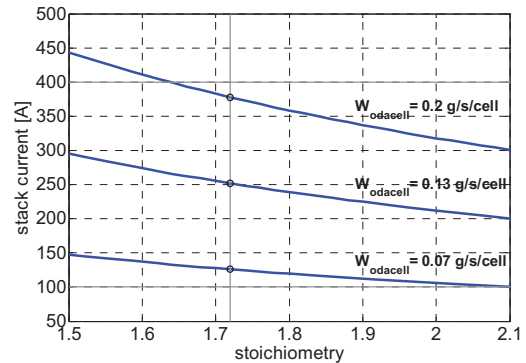


FIG 11. Stack current plotted against cathode stoichiometry to achieve an ODA cell mass flow of 0.07, 0.13 and 0.20g/s/cell; constraints are given by limits on stack current of 100-400A and minimum as well as maximum stoichiometry of 1.5 and 2.0

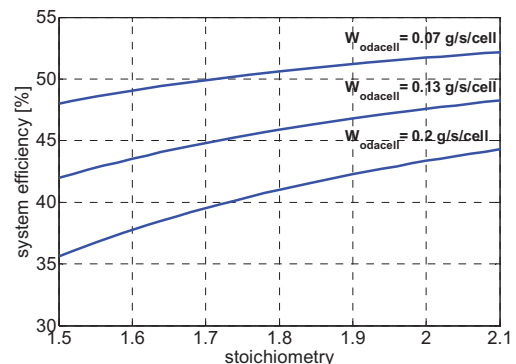


FIG 12. System efficiency over stoichiometry for ODA cell mass flows 0.07, 0.13 and 0.20g/s/cell

current less than 100A is not desirable as it could lead to flooding and therefore, stack power losses or even stack damage [13]. On the other hand, stack currents above 400A are not desirable in order to have a functioning stack inlet gas and membrane humidification. Poor stack humidification can lead to stack power losses and even stack damage [13]. The aforementioned stack current constraints are typical for this fuel cell stack. However, similar constraints can be applied to other fuel cell stacks. Further, the range for stoichiometry is constrained by a minimum and maximum limit to prevent oxygen starvation that is very likely to occur at low stoichiometry and high cathode pressures that occur for high stoichiometry.

For operation of the fuel cell system it is desirable to

operate at high efficiency to save fuel and to most effectively convert chemical energy into electrical energy. Fuel cell system efficiency (14) at each operating point has been determined through a simulation study, in which the fuel cell system was simulated at stoichiometry of 1.5 to 2.1 and stack currents as given by equation (49) to deliver dry ODA cell mass flows of 0.07, 0.13 and 0.20g/s/cell. Figure 12 shows the results. For a constant ODA mass flow, an increase in stoichiometry leads to an increase in stack efficiency. High absolute system efficiency, though, is obtained for low ODA mass flows. This effect is due to the stack current being drawn. As shown in figure 11, to generate low ODA mass flows, low stack currents are drawn. Low stack currents result in a high stack voltage. This is obvious when considering a stack polarization curve such as the exemplary one [7] shown in figure 2. The higher the stack voltage, the lower are the voltage losses and thus the more chemical energy is converted into electrical energy. So, the stack efficiency increases with decreasing stack currents. Further stoichiometry-increase is not desirable and would lead to reduction of system efficiency as the compressor power consumption increases significantly. For generation of oxygen depleted cathode exhaust gas, high system efficiency could be achieved by operating the fuel cell system at a high stoichiometry. Contrarily, ODA oxygen content rises with rising stoichiometry. Hence, to satisfy the operational constraints of keeping a 10% oxygen-content, cathode stoichiometry may not exceed an upper limit of 1.72. For lower stoichiometry the fuel cell system would operate less efficient.

4. DYNAMIC FUEL CELL SYSTEM SIMULATION MODEL AND SIMULATION RESULTS

A schematic of the entire fuel cell system consisting of the fuel cell stack, the double-loop stack cooling system with intercooler, cooler and bypass leg, cathode exhaust gas water condenser and water separators is shown in figure 13. A dynamic simulation model of the entire system has been built in Matlab/Simulink®. The stack cooling system modeled is described in [7]. A model of the intercooler has been derived based on the effectiveness NTU method.

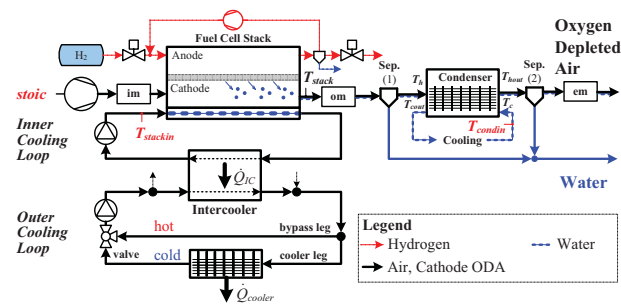


FIG 13. Entire fuel cell system: fuel cell stack, stack cooling system and condenser with separators

The nonlinear intercooler model is valid over the entire operating range of the fuel cell system. Furthermore, the nonlinear intercooler model is used for cooling controller design. A linear controller with nonlinear feedforward control actuates the cooling valve in the outer cooling loop to control for the stack cooling inlet temperature $T_{stackin}$ in the inner cooling loop. The fuel cell system model of [7] has been extended by an anode water separator model, a

static water condenser in the cathode exhaust, two water separators, and the exit manifold model. The outlet manifold model has been modeled similarly to the exit manifold model with stationary water dynamics. Model equations are given in section Stationary Fuel Cell System and Condenser Model. The condenser in the cathode exhaust line is modeled by the condenser approximation model with relaxation for faster convergence.

4.1. Condenser Model Implementation

For ODA and vapor mass flow through the condenser and the water separators equations (37), (38), (39) and (40) are utilized. The condenser outlet temperature T_{hout} is calculated with the mean pressure (26) and the approximation condenser model with relaxation for faster convergence of the solution. Vapor and liquid water outlet mass flows are obtained according to energy balance (41) and (42). However, a first order time system (51) with time constant T_{cond} for condenser ODA outlet temperature has been introduced to allow for condenser dynamic thermal behavior on the one hand and to prevent numerical problems on the other hand. T_{cond} was set small to mimic stationary behavior and to prevent numerical problems.

$$(51) T_{hout,PT1}(s) = \frac{1}{T_{cond}s + 1} T_{hout}(s)$$

Stationary energy balances of ODA (52) and cooling side (53) using $T_{hout,PT1}$ lead to cooling outlet temperature T_{cout} . The model iteration number is set to four steps.

$$(52) \begin{aligned} 0 = & W_{oda} c_{oda} T_h + W_{cond,v,in} (h_0 + c_v T_h) + W_{cond,l,in} c_l T_h \\ & - W_{oda} c_{oda} T_{hout,PT1} - W_{cond,v,out} (h_0 + c_v T_{hout,PT1}) \\ & - W_{cond,l,out} c_l T_{hout,PT1} - \dot{Q}_{cond} \end{aligned}$$

$$(53) 0 = W_{cool} c_{cool} (T_c - T_{cout}) + \dot{Q}_{cond}$$

4.2. Simulation Results

The dynamic simulation model parameters for stack voltage and mass flows have been identified as reported in [7]. The condenser is assumed to have nice cooling behavior. A heat transfer coefficient of $UA=600W/K$ as shown previously is assumed. The model is run in Matlab/Simulink®. The stack cooling inlet temperature is set to be controlled for 58°C and the condenser cooling inlet temperature is set to 5°C to lead to a high cooling effect for a high level of condensation in order to gain low ODA water loading. The stack current slope is limited to +/- 100 A/s. Aim is to efficiently operate the fuel cell system such that a certain ODA mass flow at an oxygen concentration of 10% is obtained. As discussed previously, fuel cell system efficiency would decrease when decreasing the fuel cell system stoichiometry and would increase when increasing the oxygen excess ratio. For the purpose of generating ODA conditioned with respect to oxygen content, the fuel cell system is most efficiently operated at a high stoichiometry that does not exceed the stoichiometry leading to the desired ODA oxygen content. A reference profile $W_{oda,ref} = n_{cells} \times W_{odacell,ref}$ for ODA cell mass flows of $W_{odacell,ref} = 0.07, 0.13$ and $0.20g/s/cell$ as shown in figure 14 and a reference oxygen content of $c_{O2,ref} = 10\%$ was applied to the feedforward controller derived from equations (48) and (49) with I_{stack} and λ being applied as inputs to the fuel cell system. The fuel cell

system is assumed to be perfectly tight and the mass flow controller for providing the feed air mass flow is supposed to work perfectly. Diffusion of nitrogen and oxygen through the membrane is assumed not to happen and the chemical reaction is assumed to be ideal. As shown by the simulation results in figure 14, ODA mass flow establishes fast and steady state O_2 concentration matches the reference value. However, during increasing stack current steps the oxygen content decreases as oxygen in the cathode must be replenished. For decreasing steps oxygen concentration increases as more oxygen than needed temporarily resides in the cathode.

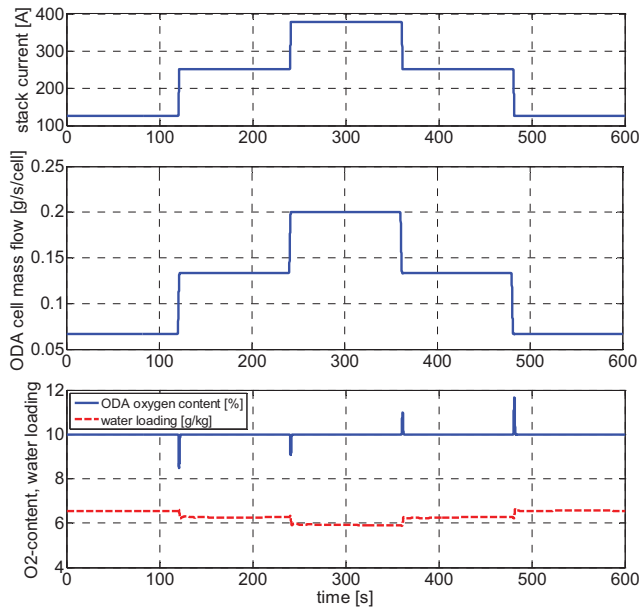


FIG 14. Simulation results: stack current profile (*top*), ODA mass flow per cell in stack (*center*) and ODA water loading and O_2 content (*bottom*)

5. CONCLUSION

A multifunctional fuel cell system is modeled and studied for inerting. Oxygen depleted cathode exhaust gas (ODA) can be used as an inert-gas due to its low oxygen content. However, ODA-gas needs to exhibit a low water loading in order to be used for inerting purposes. Depending on the choice of stack current and stoichiometry the ODA mass flow and ODA oxygen concentration can be achieved. Furthermore, water loading of ODA can be influenced by the condenser cooling temperature. However, as the amount of fuel is limited, operating the stack efficiently is highly favorable. Two opposing effects can be observed. Decreasing the cathode stoichiometry leads to the positive effect of decreasing ODA oxygen content, however, also leads to the negative effect of decreasing the stack efficiency. Increasing the stoichiometry leads to an increase in cathode pressure and therefore an increase in fuel cell stack efficiency, however, leads to an increase in ODA oxygen concentration. A stationary simulation model of the fuel cell system, water separators and water condenser is presented to analyze these effects. Moreover, a stationary condenser approximation model is derived from the stationary condenser cell model to allow for fast dynamic simulations. Based on the analysis an operating scheme for efficient fuel cell system operation is determined. This scheme is applied to a dynamic simulation model of the multifunctional fuel cell system.

6. ACKNOWLEDGMENT

This study as part of the project "cabin technology and multifunctional fuel cell systems" has been supported by Airbus and the German Federal Ministry of Education and Research (support code: 03CL03A).

7. REFERENCES

- [1] E. Vredenburg, H. Lüdders and F. Thielecke, "Methodology for Sizing and Simulation of complex Fuel Cell Systems" orig.(german) "Methodik zur Auslegung und Simulation komplexer Brennstoffzellensysteme", Deutscher Luft- und Raumfahrtkongress 2010, DocumentID: 161248.
- [2] J. Bleil, "Fuel Cells for onboard Power Supply of Aircraft", orig. (german) "Brennstoffzellen zur Bordstromversorgung von Flugzeugen", HZwei-Das Magazin für Wasserstoff und Brennstoffzellen, 04/2007
- [3] J. Niemeyer, Model Predictive Control of a PEM-Fuel Cell System, orig. (german) Modellprädiktive Regelung eines PEM-Brennstoffzellensystems, Schriften des Instituts für Regelungs- und Steuerungssysteme, Universität Karlsruhe, Band 05, 2009
- [4] J. T. Pukrushpan, A. G. Stefanopoulou and H. Peng, Control of Fuel Cell Power Systems. London: Springer-Verlag, 2004.
- [5] A. Y. Karnik, J. Sun, A. G. Stefanopoulou and J. H. Buckland, "Humidity and Pressure Regulation in a PEM Fuel Cell Using a Gain-Scheduled Static Feedback Controller", IEEE Transactions on Control Systems Technology, vol.17, No.2, pp. 283-297, 2009
- [6] D. A. McKay, W. T. Ott and A. G. Stefanopoulou, "Modeling, Parameter Identification and Validation of Reactant and Water Dynamic for a Fuel Cell Stack", Proceedings of the 2005 ASME International Mechanical Engineering Congress & Exposition, 2005
- [7] M. Schultze, M. Kirsten, S. Helmker and J. Horn, "Modeling and Simulation of a Coupled Double-Loop-Cooling System for PEM-Fuel Cell Stack Cooling", Proceedings of the UKACC 2012, Cardiff, 2012
- [8] H. D. Baehr and S. Kabelac, Thermodynamics, orig. (german) Thermodynamik, Berlin: Springer-Verlag, 2006
- [9] C. Bao, M. Ouyang and B. Yi, "Modeling and control of air stream and hydrogen flow with recirculation in a PEM fuel cell system – I. Control-oriented modeling", International Journal of Hydrogen Energy, vol. 31, pp. 1879-1896, 2006
- [10] J. C. Amphlett, R. M. Baumert, R. F. Mann, B. A. Peppley and P. R. Roberge, "Performance Modeling of the Ballard Mark IV Solid Polymer Electrolyte Fuel Cell", J. Electrochem. Soc., vol. 142, pp. 1-8, 1995
- [11] R. O'Hayre, S.-W. Cha, W. Colella and F. B. Prinz, Fuel Cell Fundamentals. Hoboken, NJ: John Wiley & Sons, 2009.
- [12] R. K. Shah and D. P. Sekulic, Fundamentals of Heat Exchanger Design, Hoboken, NJ: John Wiley & Sons, 2003
- [13] R. Borup et al., "Scientific Aspects of Polymer Electrolyte Fuel Cell Durability and Degradation", Chem. Rev., vol. 107, pp. 3904-3951, 2007